Reversal of phenotypes in *MECP2* duplication mice using genetic rescue or antisense oligos

Yehezkel Sztainberg[1,2], **Hong-mei Chen**[4,5,6], **John W. Swann**[4,5,6], **Shuang Hao**[2,6], **Bin Tang**[2,6], **Zhenyu Wu**[2,6], **Jianrong Tang**[2,6], **Ying-Wooi Wan**[2,7], **Zhandong Liu**[2,6], **Frank Rigo**[8], and **Huda Y. Zoghbi**[1,2,3,6]

[1]Department of Molecular and Human Genetics, Baylor College of Medicine, Houston, Texas 77030, USA

[2]Jan and Dan Duncan Neurological Research Institute at Texas Children's Hospital, Baylor College of Medicine, Houston, Texas 77030, USA

[3]Howard Hughes Medical Institute, Baylor College of Medicine, Houston, Texas 77030, USA

[4]The Cain Foundation Laboratories, Jan and Dan Duncan Neurological Research Institute at Texas Children's Hospital

[5]Departments of Neuroscience, Baylor College of Medicine, Houston, Texas 77030, USA

[6]Departments of Pediatrics, Baylor College of Medicine, Houston, Texas 77030, USA

[7]Department of Obstetrics and Gynecology, Baylor College of Medicine, Houston, Texas 77030, USA

[8]Isis Pharmaceuticals, 2855 Gazelle Court, Carlsbad, California 92010

Abstract

Copy number variations have been frequently associated with developmental delay, intellectual disability, and autism spectrum disorders[1]. *MECP2* duplication syndrome is one of the most common genomic rearrangements in males[2] and is characterized by autism, intellectual disability, motor dysfunction, anxiety, epilepsy, recurrent respiratory tract infections, and early death[3–5]. The broad range of deficits caused by methyl-CpG-binding protein 2 (MeCP2) overexpression poses a daunting challenge to traditional biochemical pathway-based therapeutic approaches. Accordingly, we sought strategies that directly target MeCP2 and are amenable to translation into clinical therapy. The first question, however, was whether the neurological dysfunction is reversible after symptoms set in. Reversal of phenotypes in adult symptomatic mice has been demonstrated in

some models of monogenic loss-of-function neurological disorders[6–8], including loss of MeCP2 in Rett syndrome[9], indicating that, at least in some cases, the neuroanatomy may remain sufficiently intact so that correction of the molecular dysfunction underlying these disorders can restore healthy physiology. Given the absence of neurodegeneration in *MECP2* duplication syndrome, we hypothesized that restoration of normal MeCP2 levels in *MECP2* duplication adult mice would rescue their phenotype. Therefore, we first generated and characterized a conditional *Mecp2*-overexpressing mouse model and showed that correction of MeCP2 levels largely reversed the behavioral, molecular, and electrophysiological deficits. Next, we sought a translational strategy to reduce MeCP2 and turned to antisense oligonucleotides (ASOs). ASOs are small modified nucleic acids that can selectively hybridize with mRNA transcribed from a target gene and silence it[10,11], and have been successfully used to correct deficits in different mouse models[12–18]. We found that ASO treatment induced a broad phenotypic rescue in adult symptomatic transgenic *MECP2* duplication mice (*MECP2*-TG)[19,20], and corrected *MECP2* levels in lymphoblastoid cells from *MECP2* duplication patients in a dose-dependent manner.

To determine whether *MECP2* duplication syndrome is reversible, we generated a conditional *MECP2* overexpression mouse model that carries two functional alleles with species-matched endogenous control elements: a human wild type (WT) *MECP2* allele and a conditional mouse *Mecp2* allele (*Mecp2lox*) that can be deleted using tamoxifen-inducible Cre recombination (Fig. 1a). Our breeding strategy resulted in FVB/N × C57Bl/6 F1 hybrid mice belonging to the following three genotypes: Flox, Flox;TG, and Flox;TG;Cre. The *loxP* sequences did not alter MeCP2 expression or phenotype as Flox and Flox;TG mice were indistinguishable from WT and TG mice, respectively, in both molecular and behavioral assays (Extended Data Fig. 1 and 2). To ascertain the efficiency of Cre-mediated recombination, we injected Flox;TG;Cre mice intraperitoneally with either tamoxifen (TMX) or vehicle over the course of four weeks (Fig. 1b) and euthanized four cohorts of mice at different time points after initiation of treatment. MeCP2 protein levels were significantly downregulated at 2.5 weeks, and the levels of MeCP2 remained low thereafter (Fig. 1c,d). Moreover, RT-qPCR showed that Cre-mediated recombination efficiently downregulated mRNA levels of both alternatively-spliced isoforms (*Mecp2-e1* and *Mecp2-e2*) of the floxed mouse *Mecp2*, but not the human transgenic *MECP2* allele (Fig. 1e). Finally, we confirmed the normalization of MeCP2 levels by immunofluorescence staining of hippocampal slices (Fig. 1f).

Next, we injected a new cohort of 8- to 9-week-old mice with TMX or vehicle for behavioral characterization. Flox;TG;Cre mice injected with TMX (Flox;TG;Cre-TMX) were indistinguishable from Flox control mice in the different assays, showing a resolution of the phenotypes that resemble *MECP2* duplication syndrome, such as hypoactivity, anxiety-like behavior, motor abnormalities, and social behavior deficits (Fig. 2a–f).

Changes in MeCP2 abundance affect the mRNA levels of thousands of genes in the brain[20–22]. Therefore, we hypothesized that normalizing MeCP2 levels would also normalize gene expression patterns. First, we analyzed the expression of selected MeCP2-sensitive genes in the hypothalamus[21] and the cerebellum[22] by RT-qPCR, in adult mice. The mRNA levels of these genes in the Flox;TG;Cre-TMX group were indistinguishable from

the Flox control group (Extended Data Fig. 3a,b). We then performed whole transcriptome sequencing (RNA-seq) analysis to evaluate expression patterns in the hippocampus. The analysis showed that the mRNA expression profile of the Flox;TG;Cre-TMX group clustered together with the Flox control group (Fig. 2g and Supplementary Table 1). Reducing MeCP2 to normal levels in symptomatic mice thus appears to rescue the behavioral phenotype by reversing pathogenic molecular changes in the brain.

MeCP2 levels also influence synaptic plasticity, as indicated by abnormalities in hippocampal long-term potentiation (LTP) in MeCP2 null[23] and *MECP2*-TG mice[19].

We, therefore, assessed LTP at the Schaffer collateral synapses of the CA1 area in the hippocampus, and found no difference in input/output relationship (I/O) or paired-pulse facilitation (PPF) between the groups, indicating that MeCP2 overexpression does not affect basal synaptic transmission or short-term plasticity (Extended Data Fig. 4a–d). However, normalization of MeCP2 levels in Flox;TG;Cre-TMX mice, completely rescued the abnormal, enhanced LTP (Fig. 2e,f). Defects in long-term hippocampal synaptic plasticity induced by MeCP2 overexpression are thus reversible in adult mice.

To determine whether we could normalize MeCP2 levels using a strategy that is more readily translatable into a medical therapy, we took advantage of our *MECP2*-TG mice harboring one copy of human *MECP2* (in addition to the endogenous mouse gene) to screen for a treatment using human-specific ASOs. We tested ASOs designed to bind multiple regions of the human *MECP2* pre-mRNA so as to reduce the levels of both alternatively-spliced *MECP2* isoforms, *MECP2*-e1 and *MECP2*-e2 (Extended Data Fig. 5a). After screening *MECP2*-ASOs for their ability to reduce *MECP2* levels in cultured human cells, and for toxicity in WT mice (data not shown), we screened five selected *MECP2*-ASOs by injecting them stereotaxically in the brain of *MECP2*-TG mice (Extended Data Fig. 5 and Extended Data Table 1), and used the most effective one, ASO-5, for further studies.

To determine the duration of treatment efficacy, we gradually infused ASO into the brains of 7–8-week old mice using micro-osmotic pumps designed to deliver the molecule at a constant rate over a four-week period (Fig. 3a and Extended Data Fig. 6). At the end of treatment, immunofluorescence staining showed that the ASO was widely distributed throughout the brain (Fig. 3b) and that it effectively knocked-down MeCP2 close to WT levels (Fig. 3c). We next analyzed MeCP2 expression in the cortex at different time points after initiation of treatment by western blot (as described in Fig. 3a). MeCP2 was significantly downregulated four weeks after the initiation of the treatment (Fig. 3d,e), and remained so for an additional four weeks after stopping the infusion (Fig. 3e). We further confirmed the specificity of the ASO for human *MECP2* by RT-qPCR (Fig. 3f).

We then treated a new cohort of animals for behavioral characterization. At 6–7 weeks after the initiation of the treatment, rescue was evident only in the rotarod test (Fig. 3i and Extended Data Fig. 7), but by 10–11 weeks, the hypoactivity, anxiety-like behavior and social behavior of *MECP2*-TG mice were also reversed (Fig. 3g, h, j). Ten weeks after treatment cessation, when MeCP2 levels had increased to pre-treatment levels, the symptoms reappeared (data not shown). To gain insight into the basis of the delayed

behavioral rescue, we performed RNA-seq analysis in the hippocampus at two different time points after treatment initiation (Fig. 4a and Supplementary Table 2). We found that four weeks after initiation of treatment, there was a trend towards normalization of the expression of some mRNAs, but the TG-ASO group did not cluster together with the WT group. By eight weeks, however, the TG-ASO group clustered together with the WT group, suggesting that reversal of pathogenic molecular changes in the brain as a consequence of MeCP2 normalization correlates strongly with resolution of the behavioral phenotype. To test for possible off-target effects, we compared expression profiles at both time points to detect genes whose expression was significantly affected by the ASO treatment (TG vs TG-ASO), but was not different between WT and TG mice. We found only 10 overlapping genes that meet this criterion (see Supplementary Table 2), suggesting minimal off-targets.

Seizures occur in *MECP2* duplication syndrome mice as they age[19], so we tested the ability of ASO treatment to reverse abnormal electrographic discharges in 25–35-week old *MECP2*-TG1 mice (pure FVB/N background). Vehicle-treated *MECP2*-TG1 mice manifested electrographic seizure spikes in electroencephalography (EEG) recordings from the cortex (Fig. 4b and Extended Data Fig. 8), and strong electrographic seizure events were typically accompanied by behavioral seizures (Supplementary Video 1). ASO treatment abolished these abnormal EEG discharges and eliminated behavioral seizures and electrographic seizure spikes in this group (Fig. 4b and Extended Data Fig. 8).

Lastly, we determined that *MECP2*-ASO treatment corrected *MECP2* mRNA levels in a dose-dependent manner in lymphoblastoid cells from *MECP2* duplication patients (Fig. 4c and Extended Data Table 2). The amount of ASO can thus be titrated and optimized so as to target only some *MECP2* RNA and allow translation of physiological levels of the protein.

As the main "reader" of methylated cytosines[24], MeCP2 plays a fundamental role in epigenetics, controlling chromatin states and the expression of thousands of genes[21,25,26]. Accordingly, MeCP2 expression must be maintained within a fairly narrow range to assure proper gene expression and neuronal function[27]. Here we demonstrated that restoration of MeCP2 to its normal level can largely reverse the phenotype of adult symptomatic *MECP2* duplication mice.

It is worth noting that reversal of *MECP2* duplication-like features was evident 6–7 weeks after genetic rescue but took 10–11 weeks after initiation of ASO treatment. This four-week difference is probably due to the more gradual reduction in MeCP2 levels brought about by ASO treatment. The RNA-seq results in the ASO experiment correlated nicely with the resolution of the disease phenotype: abnormal gene expression was still prominent at four weeks after the initiation of treatment (Figure 4a), whereas robust correction of gene expression eight weeks after treatment initiation (and four weeks after MeCP2 levels normalized, (Figure 3e)) was accompanied by full behavioral rescue. In mice, therefore, MeCP2 levels must be normal for one month before there is resolution of the duplication phenotypes.

The finding that ASO treatment rescues the *MECP2* duplication-like phenotypes to a similar extent of the genetic rescue provides a proof-of-concept about the value of this approach. To

move this closer to translation, further studies will have to test different ASO dosages and establish the safety margin of MeCP2 levels, using a mouse model that exclusively expresses two human *MECP2* alleles. Additionally, we will screen thousands of *MECP2*-ASOs for off-target effects.

Overall, our results show that delivering ASOs to the CNS is a promising therapeutic approach for treating *MECP2* duplication syndrome, and has potential for other disorders caused by duplication of genetic material by targeting genes in the respective critical regions, such as peripheral myelin protein 22 (*PMP22*) in Charcot-Marie-Tooth disease[28], retinoic acid induced receptor 1 (*RAI1*) in Potocki-Lupski syndrome[29], and dual specificity tyrosine-phosphorylation-regulated kinase 1A (*DYRK1A*) in Down syndrome[30].

METHODS

Antisense oligonucleotide synthesis

Isis Pharmaceuticals synthesized all ASOs as previously described[15]. All ASOs consist of 20 chemically modified nucleotides (MOE gapmer). The central gap of 10 deoxynucleotides is flanked on its 5' and 3' sides by five 2'-*O*- (2-methoxyethyl) (MOE) modified nucleotides. The backbone modifications from 5' to 3' are: 1-PS, 4-PO, 10-PS, 2-PO, and 2-PS. PS modifications were replaced with PO in the MOE wings to reduce the overall PS content of the ASO, since a fully modified PS ASO is not necessary for robust CNS activity[15]. The sequence of each ASO is listed in Extended Data Table 1.

Mice

The first MeCP2-overexpressing mice were *MECP2*-TG mice on a FVB/N pure background[19]. These mice show normal locomotion in the open field and an increase in vertical activity, which was interpreted as less anxiety, but there was no difference in anxiety-like behavior in the light-dark test. Mice on a pure FVB/N background, however, develop premature retinal degeneration, which can confound the interpretation of some behavioral tests[31]. To overcome issues related to a pure inbred strain, our laboratory characterized F1 hybrid *MECP2*-TG mice (FVB/N × C57Bl/6 or FVB/N × 129S6/SvEv) and showed that these mice display several phenotypes as early as the age of 7 weeks[20], including increased anxiety and a trend towards hypoactivity. Therefore, for both the genetic rescue and the ASO treatment experiments, we decided to continue using F1 hybrid *MECP2*-TG mice.

For experiments related to the validation of the Flox;TG mouse model (Extended Data figures 1 and 2) we generated F1 hybrid animals by mating male *MECP2*-TG1 mice on a pure FVB/N background[19] to female mice heterozygous for the *Mecp2*^lox allele (Flox) (B6;129S4-*Mecp2^{tm1Jae}*/Mmucd obtained from MMRRC, and backcrossed to C57Bl/6J for more than 10 generations; see also scheme in Extended Data Figure 1a). For experiments related to conditional rescue of *MECP2*-TG mice (Figures 1–2) we first mated Flox C57Bl/6 females with C57Bl/6 Cre-ER males (B6.Cg-Tg(UBC-cre/ERT2)1Ejb/J obtained from Jackson Laboratories). The F1 Flox;Cre females were then mated to FVB/N *MECP2*-TG1 males to generate the F1 hybrid, triple transgenic Flox;TG;Cre male mice and their control

littermates (Flox and Flox;TG) (see scheme in Figure 1a). For studies related to *MECP2*-ASOs, we generated F1 hybrid animals by mating FVB/N *MECP2*-TG1 females to wild-type 129S6/SvEv male mice (Taconic Farms). For the EEG experiment (Figure 4b) we used *MECP2*-TG1 males on a pure FVB/N background.

We routinely use mouse littermates as controls for our experiments. Throughout the experiments, mice were maintained in a temperature-controlled, AAALAS-certified Level 3 facility on a 12 hr light-dark cycle. Food and water were given *ad libitum*. All procedures to maintain and use these mice were approved by the Institutional Animal Care and Use Committee for Baylor College of Medicine.

Preparation of brain lysates and western blot

Brains were dissected and homogenized in cold lysis buffer (20mM Tris-HCl pH 8.0, 180mM NaCl, 0.5% NP-40, 1mM EDTA and Complete Protease Inhibitor, Roche, Mannheim, Germany). Lysates were rotated for 20 min at 4°C. After centrifugation at 4°C the supernatant was mixed with NuPAGE Sample Buffer, heated for 5 min at 95°C, and run on a NuPAGE 4–12% Bis-Tris gradient gel with MES SDS Running Buffer (NuPAGE, Carlsbad, CA). Proteins were transferred to a nitrocellulose membrane using NuPAGE Transfer Buffer for 1.5 hr at 4°C. The membrane was blocked for 1 hr with 5% milk in Tris-buffered saline with 2% Tween-20 (TBST) followed by overnight incubation with primary antibody at 4°C. After 4 washes of 10 min each with TBST, the membrane was incubated with secondary antibody for 1–2 hrs at room temperature. HRP was detected using SuperSignal West Dura kit, Thermo Scientific, IL, USA. Western blot images were acquired by ImageQuant LAS 4000 (GE Healthcare) and quantified by an ImageJ software package. Primary antibodies: rabbit antiserum raised against the N-terminus of MeCP2 (1:5,000; Zoghbi lab, #0535), mouse anti-GAPDH 6C5 (1:20,000; Advanced Immunochemicals, 2-RGM2, Long Beach, CA, USA). Secondary antibodies: goat anti-rabbit HRP (1:20,000; Bio-Rad, #170-5046, Hercules, CA, USA), donkey anti-mouse HRP (1:20,000; Jackson ImmunoResearch Labs, 715-035-150, West Grove, PA).

Gene expression analysis by RT-qPCR

The subset of mice for RTqPCR was selected randomly, using Excel software to generate a table of random numbers. No significant differences on behavioral measurements were found between the selected mice and the rest (per genotype group). Total RNA from mouse brain tissue was extracted using miRNeasy minikit (Qiagen, Hilden, Germany), and 1 μg of total RNA was used to synthesize cDNA by Quantitect reverse transcription kit (Qiagen). For human lymphoblasts 2μg of total RNA was used to synthesize cDNA. RT-qPCR was performed in a CFX96 Real-Time System (Bio-Rad, Hercules, CA, USA) using PerfeCTa SYBR Green Fast Mix (Quanta Biosciences, Gaithersburg, MD, USA). Sense and antisense primers were selected to be located on different exons, and the RNA was treated with DNase, to avoid false-positive results caused by DNA contamination. The specificity of the amplification products was verified by melting curve analysis. All RT-qPCR reactions were conducted in technical triplicates and the results were averaged for each sample, normalized to *Hprt* levels, and analyzed using the comparative ddCt method. The following primers were used in the RT-qPCR reactions: *MECP2* (common to human and mouse): 5'-

TATTTGATCAATCCCCAGGG-3' (sense) 5'-CTCCCTCTCCCAGTTACCGT-3' (antisense); *MECP2* (human specific): 5'-GATGTGTATTTGATCAATCCC-3' (sense) 5'-TTAGGGTCCAGGGATGTGTC-3'; *Mecp2-e1* (mouse specific): 5'-AGGAGAGACTGGAGGAAAAGTC-3' (sense) 5'-CTTAAACTTCAGTGGCTTGTCTCTG-3' (antisense); *Mecp2-e2* (mouse specific): 5'-CTCACCAGTTCCTGCTTTGATGT-3' (sense) 5'-CTTAAACTTCAGTGGCTTGTCTCTG-3' (antisense); *MECP2-e1* (human specific): 5'-AGGAGAGACTGGAAGAAAGTC-3' (sense) 5'-CTTGAGGGGTTTGTCCTTGA-3' (antisense); *MECP2-e2* (human specific): 5'-CTCACCAGTTCCTGCTTTGATGT-3' (sense) 5'-CTTGAGGGGTTTGTCCTTGA-3' (antisense); *Hprt* (mouse specific): 5'-CGGGGGACATAAAAGTTATTG-3' (sense) 5'-TGCATTGTTTTACCAGTGTCAA-3' (antisense); *HPRT* (human specific): 5'-GACCAGTCAACAGGGGGACAT-3' (sense) 5'-CCTGACCAAGGAAAGCAAAG-3' (antisense); *Sst*: 5'-CCCAGACTCCGTCAGTTTCT-3' (sense) 5'-GAAGTTCTTGCAGCCAGCTT-3' (antisense); *Crf*: 5'-TACCAAGGGAGGAGAAGAGA-3' (sense) 5'-GATCAGAACCGGCTGAGGT-3' (antisense); *Npbwr1*: 5'-TCTCTTACTTCATCACCAGCC-3' (sense) 5'-GCATAGAGGAAAGGGTTGAG-3' (antisense); *Gamt*: 5'-GGATTATTGAGTGCAATGATGG-3' (sense) 5'-TCAAGGGAACAACCTTATGTG-3' (antisense); *Agrp*: 5'-TCAAGAAGACAACTGCAGAC-3' (sense) 5'-TCTGTGGATCTAGCACCTC-3' (antisense); *Rcor2*: 5'-ACCCGAAGTCGAACTAGTG-3' (sense) 5'-CTAGTTCATCACTGTCTTCTTTG-3' (antisense); *Prl2c2*: 5'-CATGAGCACCATGCTTCAG-3' (sense) 5'-GCGAGCATCTTCATTGTCAG-3' (antisense).

Immunofluorescence

Animals were anesthetized with a mix of ketamine 37.6 mg/ml, xylazine 1.92 mg/ml and acepromazine 0.38 mg/ml, and transcardially perfused with 20 ml phosphate-buffered saline (PBS) followed by 100 ml of cold PBS-buffered 4% paraformaldehyde (PFA). The brains were removed and post-fixed overnight in 4% PFA. Next, brains were cryoprotected in 4% PFA with 30% sucrose at 4°C for two additional days and embedded in Optimum Cutting Temperature (O.C.T., Tissue-Tek, VWR, Radnor, PA, USA). Free-floating 40μm brain sections were cut using a Leica CM3050 cryostat and collected in PBS. The sections were blocked for 1hr in 2% normal goat serum, 0.3% TritonX-100 in PBS at room temperature. Sections were then incubated overnight at 4°C with either rabbit anti-MeCP2 (1:1,000; Cell Signaling, D4F3, Danvers, MA, USA) or rabbit anti-ASO (1:10,000; Isis Pharmaceuticals, CA, USA). The sections were washed three times for 10 min with PBS and incubated for 3hrs at room temperature with goat anti-rabbit (1:500; Alexa Fluor 488, Invitrogen, A-11034, Carlsbad, CA, USA). Sections were washed again three times for 10 min with PBS and mounted onto glass slides with Vectashield mounting medium with DAPI (Vector Laboratories, Burlingame, CA, USA).

Tamoxifen treatment

Tamoxifen (Sigma-Aldrich, T5648, St. Louis, MO, USA) was dissolved to 20 mg/ml in peanut oil, aliquotted and frozen at −20°C until use. Peanut oil was also used as vehicle.

Tamoxifen or vehicle was injected intraperitoneally at a dose of 100 mg/kg, 3 alternative days a week for 4 weeks (as described in Figure 1b).

Behavioral assays

All data acquisition and analyses were carried out by an individual blinded to the genotype and treatment. All behavioral studies were performed during the light period. Mice were habituated to the test room for 1 hr before each test. At least one day was given between assays for the mice to recover. All the tests were performed as previously described[23] with few modifications.

Open field

After habituation in the test room (150 lx, 60 dB white noise), mice were placed in the center of an open arena ($40 \times 40 \times 30$ cm), and their behavior was tracked by laser photobeam breaks for 30 min. General locomotor activity was automatically analyzed using AccuScan Fusion software (Omnitech, Columbus, OH, USA) by counting the number of times mice break the laser beams (activity counts). In addition, rearing activity, time spent in the center of the arena, entries to the center and distance traveled were analyzed. In this study we found that *MECP2*-TG mice are hypoactive in the open field test. In contrast, in *Samaco et al., Nat Genet 2012, MECP2*-TG mice show a non-significant trend towards hypoactivity. This difference might be the result of our study assessing locomotor activity by measuring activity counts, and *Samaco et al., Nat Genet 2012* by measuring the distance traveled, which is calculated by the software from the activity counts.

Elevated plus maze

After habituation in the test room (700 lx, 60 dB white noise), mice were placed in the center part of the maze facing one of the two open arms. Mouse behavior was video-tracked for 10 min and the time mice spent in the open arms and the entries to the open arms, as well as the distance traveled in the open arms, were recorded and analyzed using ANY-maze system (Stoelting, Wood Dale, IL, USA).

Accelerating rotarod

After habituation in the test room (700 lx, 60 dB white noise), motor coordination was measured using an accelerating rotarod apparatus (Ugo Basile, Varese, Italy). Mice were tested for 2 consecutive days, 4 trials each, with an interval of 60 min between trials to rest. Each trial lasted for a maximum of 10 min and the rod accelerated from 4 to 40 r.p.m. in the first 5 min. The time that it took for each mouse to fall from the rod (latency to fall) was recorded.

Three-Chamber test

The three-chamber apparatus consists of a clear Plexiglas box ($24.75 \times 16.75 \times 8.75$) with removable partitions that separate the box into three chambers. In both left and right chambers a cylindrical wire cup was placed with the open side down. Age and gender-matched C57Bl/6 mice were used as novel partners. Two days before the test, the novel partner mice were habituated to the wire cups (3 inches diameter by 4 inches in height) for 1

h per day. After habituation in the test room (700 lx, 60 dB white noise), mice were placed in the central chamber and allowed to explore the 3 chambers for 10 min (habituation phase). Next, a novel partner mouse was placed into a wire cup in either the left or the right chamber. An inanimate object was placed as control in the wire cup of the opposite chamber. The location of the novel mouse was randomized between left and right chambers across subjects to control for side preference. The mouse tested was allowed to explore again for an additional 10 min. The time spent investigating the novel partner (defined by rearing, sniffing or pawing at the wire cup) and the time spent investigating the inanimate object were measured manually.

RNA-seq

Mice were euthanized under anesthesia and the hippocampi were quickly dissected over ice. Total RNA of 30 hippocampal samples (three biological replicates of each genotype from three experiments) was extracted using miRNeasy minikit (Qiagen, Hilden, Germany), following the manufacturer's instructions. Isolated RNA was eluted in RNase-free water and submitted to the Genomic and RNA Profiling Core at Baylor College of Medicine. Sample quality checks using the NanoDrop spectrophotometer and Agilent Bioanalyzer 2100 were conducted. Then Illumina TruSeq RNA library preparation protocol was used as follows: A double-stranded DNA library was created using 250 ng of total RNA (measured by picogreen), preparing the fragments for hybridization onto a flow-cell. First, cDNA was created using the fragmented 3' poly(A) selected portion of total RNA and random primers. During second strand synthesis, dTTP is replaced with dUTP which quenches the second strand during amplification, thereby achieving strand specificity. Libraries were created from the cDNA by first blunt ending the fragments, attaching an adenosine to the 3' end and finally ligating unique adapters to the ends. The ligated products were then amplified using 15 cycles of PCR. The resulting libraries were quantitated using the NanoDrop spectrophotometer and fragment size assessed with the Agilent Bioanalyzer. A qPCR quantitation was performed on the libraries to determine the concentration of adapter ligated fragments using Applied Biosystems ViiA7 Real-Time PCR System and a KAPA Library Quant Kit. Using the concentration from the ViiA7 qPCR machine, 21pM of library was loaded onto a flowcell and amplified by bridge amplification using the Illumina cBot machine. A paired-end 100 cycle run was used to sequence the flow-cell on a HiSeq Sequencing System.

RNA-Seq Data Pre-processing and Analysis

For each sample, about 10 million of 100 bp pair-end reads were generated. Raw reads were first groomed by removing adapters from both the 3'- and 5'-ends before mapping to reference genome. Then, trimmed reads were aligned to the *Mus musculus* genome (UCSC *mm10*; the gene model for the mapping was obtained from http://tophat.cbcb.umd.edu/igenomes.html) using TopHat v2.0.9[32] with default parameters (*-r 200 –p 5*). The mappability for all 30 samples was above 85%. To prepare the aligned sequence reads into expression level for differential gene analysis, we employed the free Python program HTSeq[33]. The *htseq-count* function of HTSeq allowed us to accumulate the number of aligned reads that fall under the exons of the gene (union of all the exons of the gene). These read counts are analogous to the expression level of the gene. Using the obtained read

counts, differential gene analyses were carried out using the DESeq package and *glm.nb* function in the R environment. DESeq includes functions for us to normalize the read counts of multiple samples across multiple genotypes by the use of the negative binomial distribution and a shrinkage estimator for the distribution's variance[34]. *glm.nb* allows us to fit a negative binomial regression model to test the gene changes between genotypes. Specifically, for data from the ASO experiment, each gene was tested to check if its expression levels in WT and TG-ASO mice differed from that in TG mice. Similarly, for data from the genetic rescue experiment, expression levels in Flox and Flox;TG;Cre-TMX were tested for differences from the expression in Flox;TG;Cre-vehicle and Flox;TG. The statistical significance of the observed changes was reported by the false discovery rate (FDR), which is the p-value adjusted for multiple testing with the Benjamini-Hochberg procedure. A gene was considered significantly different between genotypes if it fell under a FDR of 10% and changed in a coherent direction.

Sample Clustering

To assess the similarity of expression patterns between samples of different genotypes, we carried out unbiased clustering: expressions of the identified significantly changed genes were clustered by sample based on Euclidean distance on average linkage and by genes based on Euclidean distance on complete linkage. Heatmaps were then used to plot the clustered gene expressions for visual inspection. The plotted expressions (z-scores) for each gene were the expressions normalized at the gene level to have an average of zero and a standard deviation of one.

Hippocampal slice preparation

Mice were deeply anesthetized with isofluorane, followed by decapitation. The brain was removed into oxygenated and ice-cold cutting solution (CS) containing (in mM): 110 sucrose, 60 NaCl, 3 KCl, 1.25 NaH_2PO_4, 28 $NaHCO_3$, 0.5 $CaCl_2$, 7 $MgCl_2$, 5 glucose, and the caudal portion of the forebrain containing the hippocampus and entorhinal cortex was isolated by razor blade cuts. Transverse slices (400 μm) were prepared with a Vibratome (Viratome, St Louis, MO, USA). Cortical tissue was then removed and hippocampal slices were equilibrated in a mixture of 50% CS and 50% artificial cerebrospinal fluid (ACSF) containing (in mM): 125 NaCl, 1.25 NaH_2PO_4, 2.5 KCl, 25 $NaHCO_3$, 2 $CaCl_2$, 1 $MgCl_2$, 15 glucose, at room temperature for 10 to 20 min prior to transfer to the recording chamber.

Slice electrophysiology

All data acquisition and analysis were carried out blinded to the genotype and treatment. Electrophysiology was performed in an interface chamber (Fine Science Tools, Foster City, CA, USA). Oxygenated ACSF (95%/5% O_2 /CO_2, 31°C) was perfused into the recording chamber at the rate of 1.5 mL/min. Electrophysiological traces were digitized and stored using a Digidata 1320A and Clampex software (Axon Instruments, Union City, CA, USA). Field EPSPs (fEPSPs) were recorded in the stratum radiatum with an ACSF-filled glass recording electrode (1–3 MΩ). The relationship between fiber volley amplitude and fEPSP slope over various stimulus intensities was used to assess baseline synaptic transmission. All subsequent experimental stimuli were set to an intensity that evoked a 30%–40% of the maximal fEPSP slope. Slices that did not exhibit stable fEPSP slopes during the first 20 min

of recording were excluded from the analysis. Paired-pulse facilitation was measured at varying interstimulus intervals (20, 50, 100, 200, and 300 ms). LTP was induced by 2 trains of high-frequency stimulation (HFS, 100 Hz for 1 s) with 20 s intertrain interval. Synaptic efficacy was monitored for 20 min prior to and 70 min following LTP induction by recording fEPSPs every 20 s (3 traces were averaged over succeeding 1 min intervals). For the quantification of the last ten minutes of the LTP recording (Figure 2f), slices were averaged per mouse and statistical analysis was done on the animals (n = 6–7 mice/15–20 slices, two-tailed t-test).

Intracerebral injection of ASO

Mice were anesthetized with isoflurane and placed on a computer-guided stereotaxic instrument (Angle Two Stereotaxic Instrument, Leica Microsystems, Bannockburn, IL, USA) that is fully integrated with the Franklin and Paxinos[35] mouse brain atlas through a control panel. Anesthesia (isoflurane 3%) was continuously delivered via a small face mask. Ketoprofen 5mg/kg was administered subcutaneously at the initiation of the surgery. After sterilizing the surgical site with betadine and 70% alcohol, a midline incision was made over the skull and a small hole was drilled through the skull above the right lateral ventricle. A total of 500µg *MECP2*-ASO or saline was delivered using a Hamilton syringe connected to a motorized nanoinjector at 0.3µl min^{-1}. The coordinates used relative to bregma were: AP = −0.2 mm, ML = 1 mm, DV = −3 mm, based on a calibration study indicating these coordinates as leading to the right ventricle in our mice. To allow diffusion of the solution into the brain, the needle was left for 5 min on the site of injection. The incision was manually closed with suture. Carprofen-containing food pellets were provided for 5 days after the surgery. Two weeks after the surgery the animals were sacrificed and their brains dissected for RNA and protein analysis.

Surgical implantation of cannula and osmotic pumps

Two days before surgery, a micro-osmotic pump (Alzet model 1004, Durect, Cupertino, CA, USA) was filled with 500µg *MECP2*-ASO or Control-ASO dissolved in 100µl saline. The pump was then connected through a plastic catheter to a cannula (Alzet Brain Infusion Kit 3, Durect, Cupertino, CA, USA) (See Extended Data Figure 6a). The pump was designed to deliver the drug at a rate of 0.11µl per hour for 28 days. The cannula + pump assembly was primed in sterile saline for two days at 37°C. Mice were anesthetized with isoflurane and placed on a computer-guided stereotaxic instrument (Angle Two Stereotaxic Instrument, Leica Microsystems, Bannockburn, IL, USA). Anesthesia (isoflurane 3%) was continuously delivered via a small face mask. Ketoprofen 5mg/kg was administered subcutaneously at the initiation of the surgery. After sterilizing the surgical site with betadine and 70% alcohol, a midline incision was made over the skull and a subcutaneous pocket was generated on the back of the animal. Next, the pump was inserted into the pocket and the cannula was stereotactically implanted to deliver the drug in the right ventricle using the following coordinates: AP = −0.2 mm, ML = 1 mm, DV = −3 mm. The incision was sutured shut. Carprofen-containing food pellets were provided for 5 days after the surgery. The pump was disconnected and removed 28 days after the initiation of treatment. Two additional weeks were given to the animals to recover before any behavioral testing.

EEG monitoring

Mice were anesthetized with isoflurane and mounted in a stereotaxic frame. Under aseptic conditions, each mouse was surgically implanted with three recording electrodes (Teflon-coated silver wire, 125 μm in diameter) aimed at the subdural space of left frontal cortex, left parietal cortex, and right parietal cortex. The reference electrode was then positioned in the occipital region of the skull. All electrode wires were attached to a miniature connector (Harwin Connector). After 3–5 days of post-surgical recovery, cortical electroencephalogram (EEG) activity (filtered between 0.5 Hz and 5 kHz, sampled at 2 kHz) and behavior were simultaneously recorded in freely moving mice for 2 hour per day over 3–5 days[36].

EEG data analysis

All the EEG recordings were qualitatively and manually analyzed by experimenters blind to the mouse genotype and treatment. Electrographic seizure activities were visually identified and matched with the behavioral seizure, if there was. Other abnormal epileptiform spikes were also identified visually[37].

Lymphoblasts culture and transfection with ASOs

Following informed consent, approved by the Institutional Review Board for Human Subject Research at Baylor College of Medicine, a venous blood sample was provided by 5 individuals affected with *MECP2*-duplication syndrome and 5 age-matched controls in order to establish immortalized B-lymphoblastoid cell lines, following standard procedures. Human B-lymphoblastoid cells were cultured in suspension in RPMI 1640 medium with L-glutamine, penicillin-streptomycin, and 10% (vol/vol) fetal bovine serum. A day before transfection, cells were seeded in 6-wells plates at a density of 1×10^6 cells in a total volume of 2 ml complete medium. Transfection mixture was prepared by combining 20 μl ASO (at the desire concentration), 4 μl transfection reagent (TurboFect, R0531, Thermo Scientific) and 180 μl serum free RPMI medium. The mix was incubated at room temperature for 15 minutes before adding to the cells. RNA was extracted from lymphoblasts 48 hrs following transfection. Lymphoblastoid cells from the age-matched control donors and the non-treated *MECP2* duplication cells were incubated with 4.8 μM Control-ASO.

Statistical analysis

Statistical significance was analyzed using GraphPad Prism. The number of animals used (n), and the specific statistical tests used are indicated for each experiment in the figure legends. Sample size in behavioral studies was based on previous reports using transgenic mice with the same background. Mice were randomly assigned to vehicle or treatment groups using Excel software to generate a table of random numbers, and the experimenter was always blind to the treatment. For behavioral assays, all population values appear normally distributed. Equal variances were never assumed, and the Geisser-Greenhouse correction for sphericity was always applied when using ANOVA.
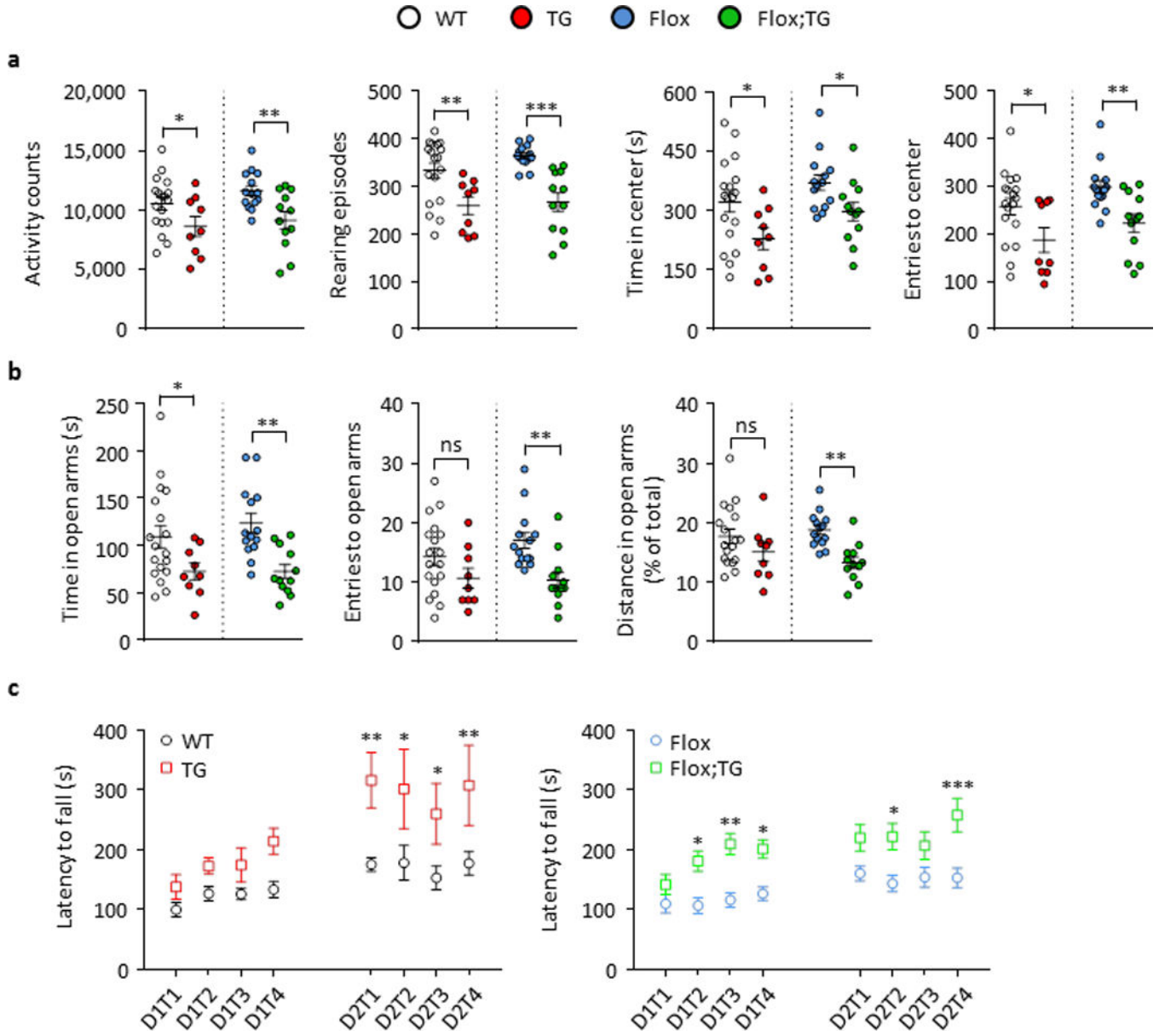
Extended Data
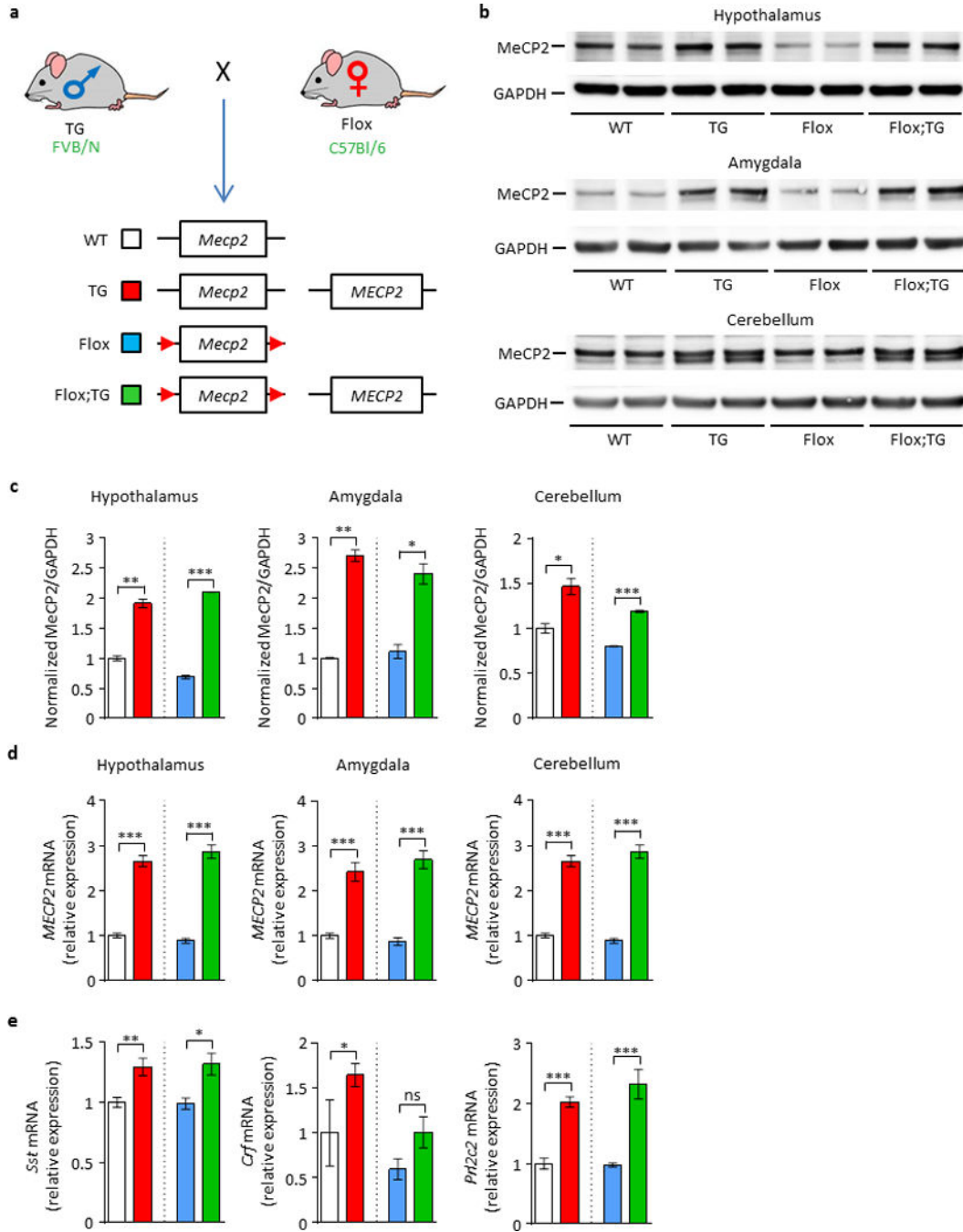
Extended Data figure 1. Mice that overexpress a human *MECP2* transgene over a floxed *Mecp2* allele resemble the classic *MECP2*-TG mice at the molecular level

a, Breeding strategy to generate mice that have a WT *MECP2* allele and a *Mecp2* allele flanked by *loxP* sequences. **b**, Western blot of MeCP2 in hypothalamus, amygdala and cerebellum. GAPDH was used as the internal control (for gel source data, see Supplementary Figure 3). **c**, Densitometry analysis of western blots in **b**). Flox;TG mice overexpress MeCP2 at levels similar to TG mice. It is noteworthy that in the hypothalamus

Flox mice were 30% hypomorphic (n = 2 mice per group, two-tailed *t*-test) when compared to WT mice, but not in the other regions. **d**, RT-qPCR analysis in hypothalamus, amygdala and cerebellum, using common primers to mouse and human *MECP2*. Flox;TG mice overexpressed the *MECP2* transcript at levels similar to TG mice. *Hprt1* was used as the internal control (n = 5 mice per group, two-tailed *t*-test). **e**, RT-qPCR analysis of three selected genes know to be altered by MeCP2 overexpression. Flox;TG mice overexpressed the *Sst, Crf and Prl2c2* transcripts at levels similar to those of TG mice. *Hprt1* was used as the internal control (n = 4 for WT, n = 6 for TG, n = 5 for Flox and Flox;TG groups, two-tailed *t*-test). ns, not significant. Data are presented as mean ± s.e.m. *P< 0.05; ** P< 0.01; ***P< 0.001.

Extended Data figure 2. Mice that overexpress a human *MECP2* transgene over a floxed *Mecp2* allele show characteristic behavioral deficits

a, Flox;TG mice displayed hypoactivity and anxiety in the open field test similar to TG mice. **b**, Flox;TG mice showed heightened anxiety-like behavior in the elevated plus maze test. **c**, Flox;TG mice showed enhanced motor learning in the rotarod test similar to TG mice. n = 18 for WT group; n = 9 for TG group; n = 14 for Flox group; n = 12 for Flox;TG group (for all behavioral tests). Data were analyzed by one-way ANOVA. Rotarod was analyzed by two-way ANOVA repeated measures followed by Tukey HSD *post hoc* correction for multiple comparisons. ns, not significant. Data are presented as mean ± s.e.m. *$P < 0.05$; ** $P < 0.01$; ***$P < 0.001$.
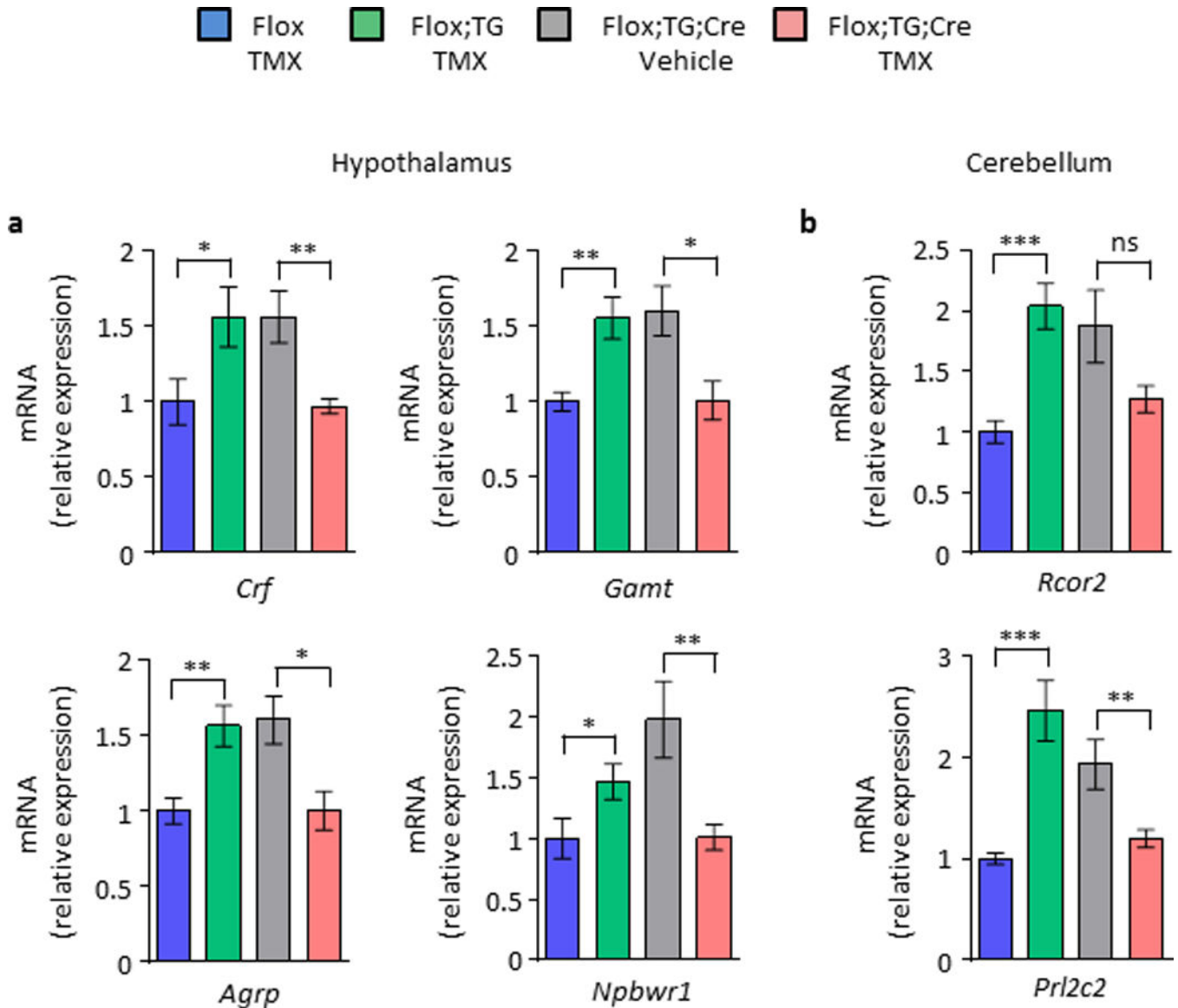
Extended Data figure 3. Correction of gene expression after genetic rescue

a-b RT-qPCR from hypothalamus (**a**) and cerebellum (**b**) shows correction of altered expression of selected genes upon normalization of MeCP2 levels in Flox;TG;Cre-TMX

mice. (n = 6 for Flox, n = 7 for Flox;TG, n = 7 for Flox;TG;Cre-vehicle, n = 8 for Flox;TG;Cre-TMX, two-tailed *t*-test). ns, not significant. Data are presented as mean ± s.e.m. *$P < 0.05$; ** $P < 0.01$; ***$P < 0.001$.
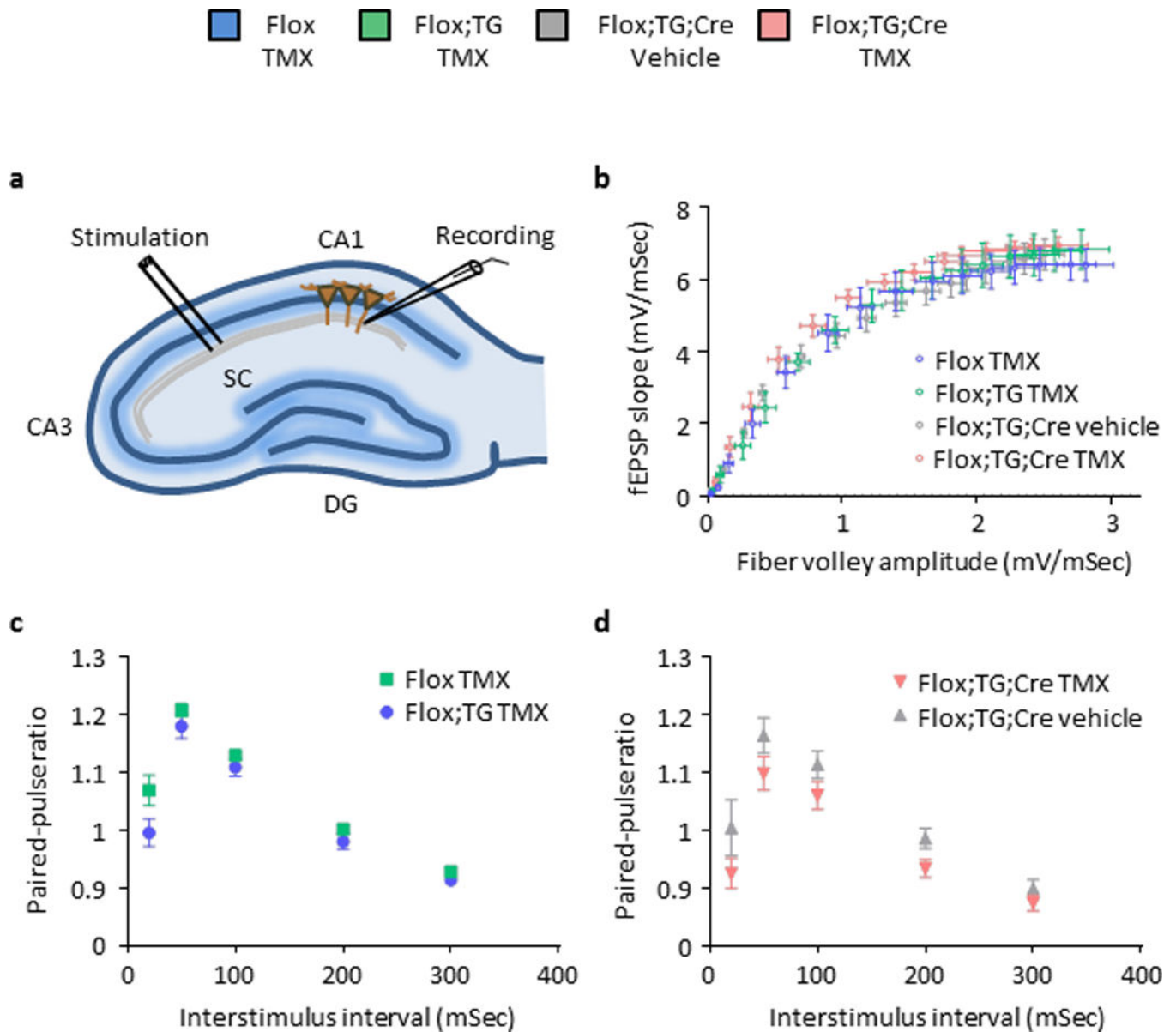
Extended Data figure 4. Hippocampal basal synaptic transmission and short-term synaptic plasticity are normal in *MECP2*-TG mice

a, Long-term potentiation was induced by applying high-frequency stimulation to the Schaffer collateral axons, and field EPSPs (fEPSPs) were recorded at the Schaffer collateral-CA1 synapses of the hippocampus (stratum radiatum). **b**, MeCP2 overexpression did not affect Schaffer collateral basal synaptic transmission, as determined by the correlation between the slopes of the evoked field excitatory synaptic potentials (fEPSPs) and the amplitudes of the fiber volleys. **c–d**, MeCP2 overexpression did not affect short-term synaptic plasticity, as determined by paired-pulse facilitation (n = 7 for Flox, n = 6 for

Flox;TG, n = 7 for Flox;TG;Cre-vehicle, n = 7 for Flox;TG;Cre-TMX). Data are presented as mean ± s.e.m.
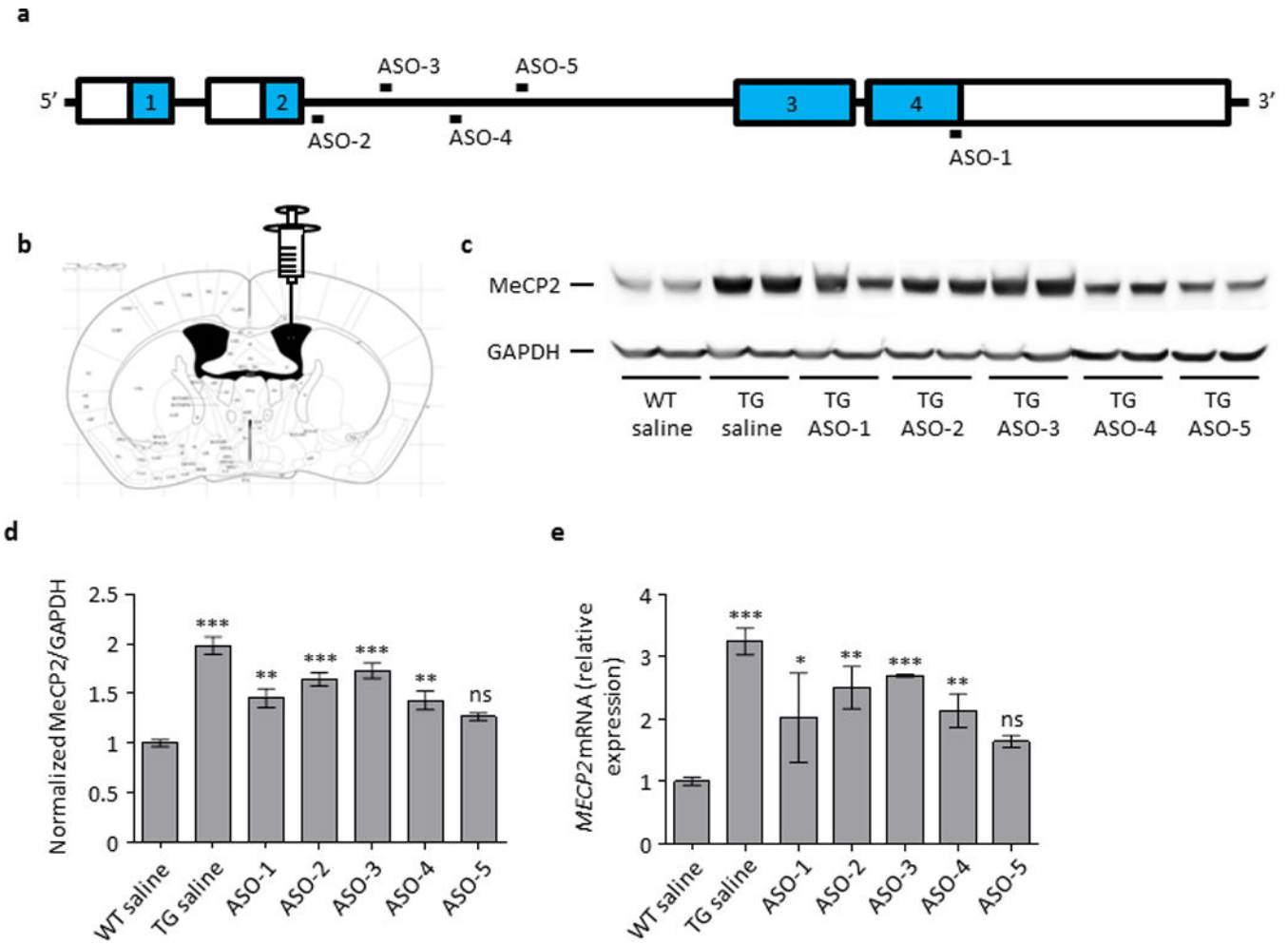
Extended Data figure 5. ASO-5 reduces *MECP2* mRNA and protein levels
a, Location of ASOs-targeting sequences on the *MECP2* pre-mRNA. Boxes represent exons and lines are introns. Boxes in blue denote the translatable regions. **b**, Section schemata from the Paxinos and Franklin[35] mouse brain atlas showing site of stereotactic injection. **c**, Western blot and densitometric analysis (**d**) of MeCP2 from cortical samples of mice treated with saline or the indicated ASOs two weeks after single bolus stereotactic injection of 500 µg ASO in the right ventricle of the brain. ASO-5 was found to be the most effective. GAPDH was used as an internal control (n = 3, one-way ANOVA followed by Tukey HSD *post-hoc* correction for multiple comparisons; for gel source data, see Supplementary Figure 4). **e**, RT-qPCR analysis of *MECP2* mRNA from cortical samples of mice treated with saline or the indicated ASOs, two weeks after single bolus stereotaxic injection of 500 µg ASO in the right ventricle of the brain. ASO-5 was found to be the most effective. The *MECP2* primers are common to the mouse and human alleles. *Hprt1* was used as an internal control (n = 3, one-way ANOVA followed by Tukey HSD *post hoc* correction for multiple

comparisons). ns, not significant. Data are presented as mean ± s.e.m. *$P < 0.05$; ** $P < 0.01$; ***$P < 0.001$.
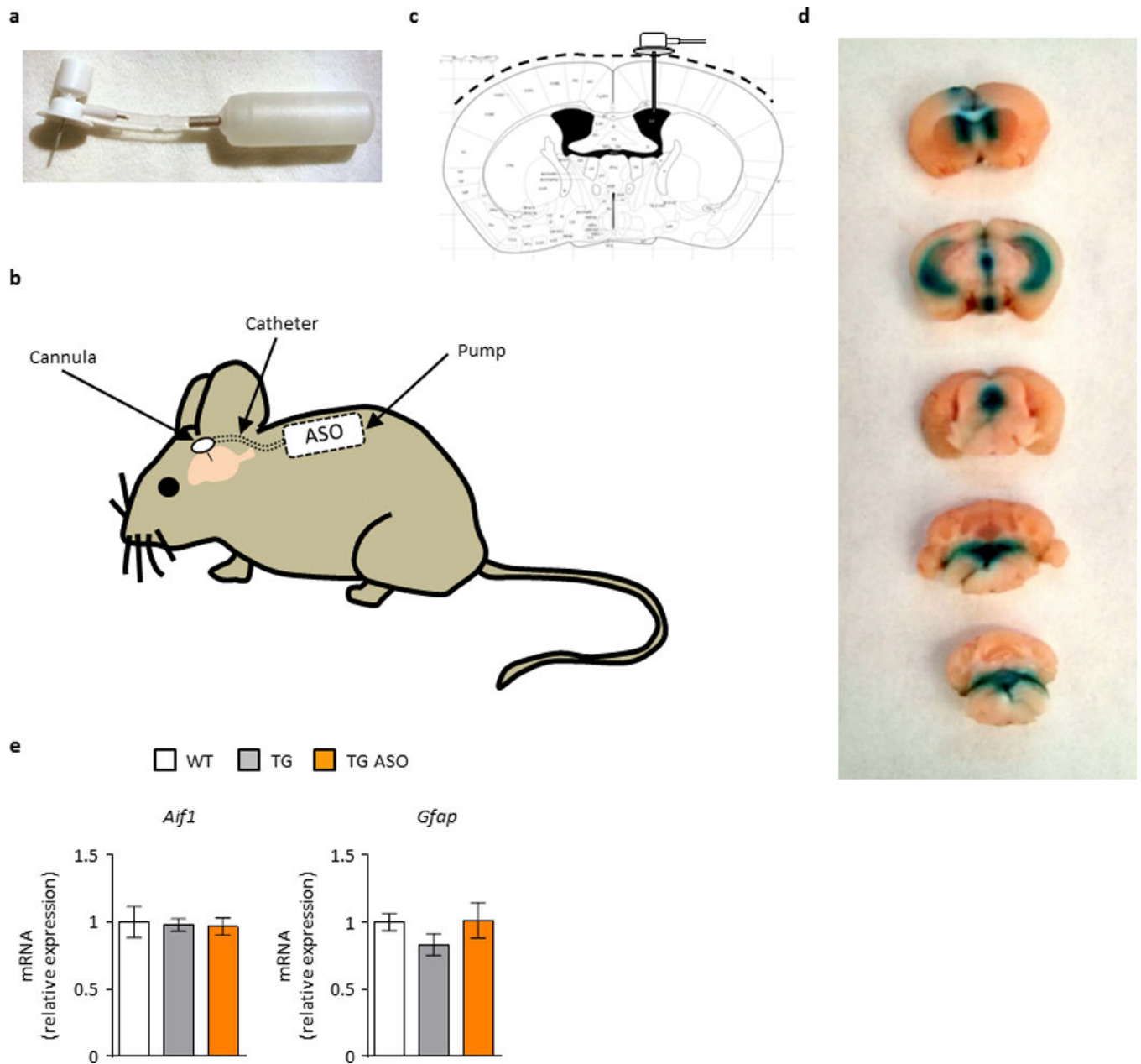
**Extended Data figure 6. Osmotic micro-pumps for gradual intracerebroventricular infusion of ASO**

a, Micro-osmotic pump connected to a cannula through a plastic catheter. **b**, The micro-osmotic pump was implanted in a subcutaneous pocket and the cannula stereotaxically positioned to deliver the ASO into the right ventricle. **c**, Section schemata from the Paxinos and Franklin[35] mouse brain atlas showing site of cannula implantation. **d**, Injection of 1 μl of dye through the catheter to show that the dye reaches the whole ventricular system, confirming the correct positioning of the tip of the cannula in the right ventricle. **e**, RT-qPCR

for *Aif1* (a marker of activated microglia) and *Gfap* (a marker of astrocytes) immediately after the end of 4 weeks gradual ASO treatment (n = 4 for WT, n = 5 for TG, n = 4 for TG-ASO). Data are presented as mean ± s.e.m.
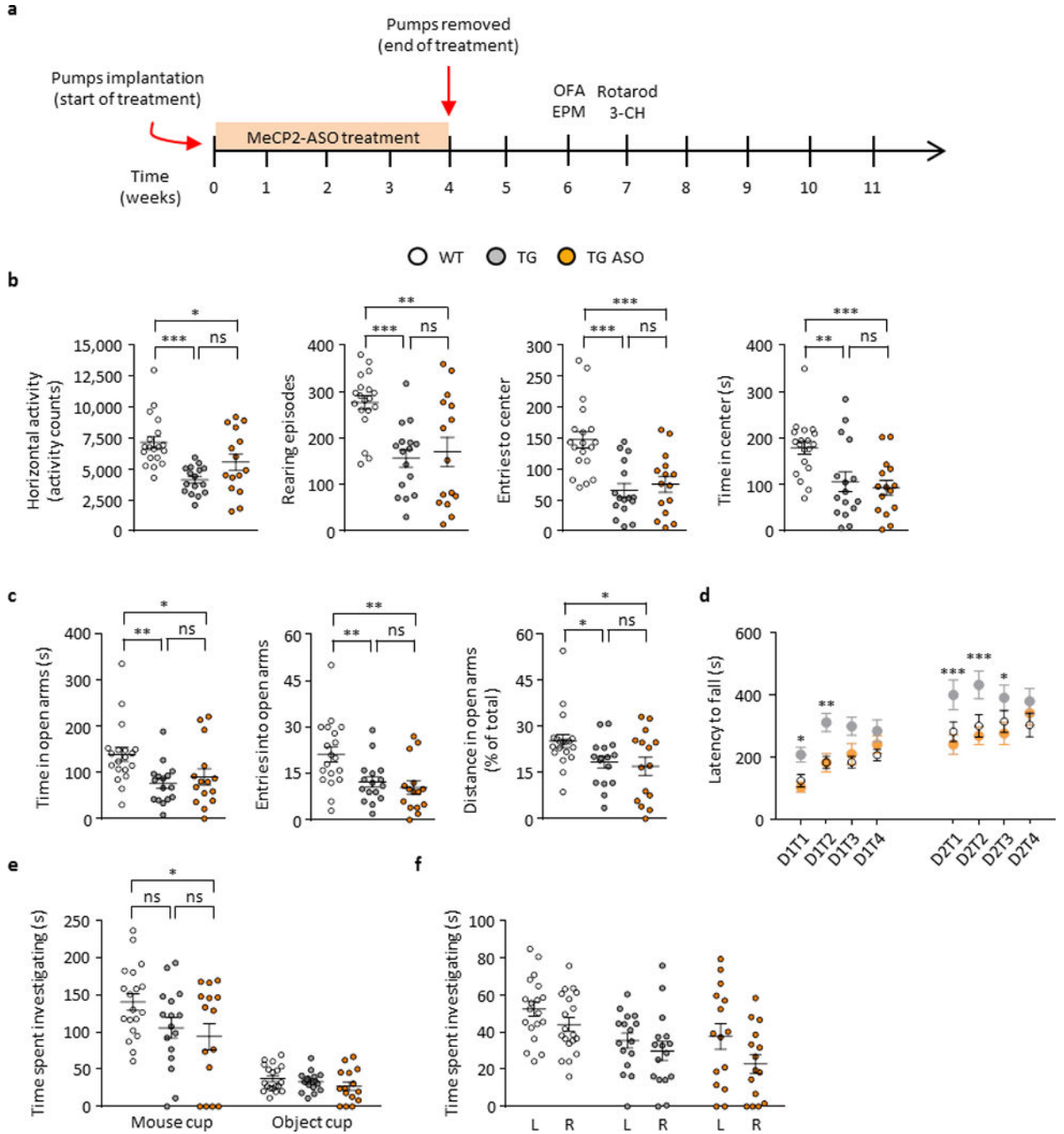
Extended Data figure 7. Behavioral phenotype 6–7 weeks after the initiation of ASO treatment
a, Timeline of ASO treatment and behavioral tests. OFA, open field activity test; EPM, elevated plus maze test; 3-CH, 3 chamber social interaction test. **b**, Two weeks after cessation of ASO treatment, *MECP2*-TG mice showed no rescue of hypoactivity, rearing

behavior or anxiety parameters in the open field. **c**, No rescue was evident in any of the parameters of the elevated plus maze test at this early post-treatment stage. **d**, ASO treatment normalized performance in the rotarod test in *MECP2*-TG mice (asterisks indicate significance between *MECP2*-TG ASO-ctrl and *MECP2*-TG ASO groups). **e**, The impaired social behavior in the 3-chamber test was not normalized in the ASO treated group. No significant difference was found between any of the groups in the time spent investigating the inanimate object. **f**, No preference for the cups placed in the left or right chambers was found in the habituation phase of the 3-chamber test. n = 19 for WT group; n = 16 for TG group; n = 15 for TG-ASO group (for all behavioral tests). Data were analyzed by one-way ANOVA followed by Fisher's LSD *post hoc* test. Rotarod was analyzed by two-way ANOVA repeated measures followed by Tukey HSD *post hoc* correction for multiple comparisons. ns, not significant. Data are presented as mean ± s.e.m. *$P < 0.05$; ** $P < 0.01$; ***$P < 0.001$.
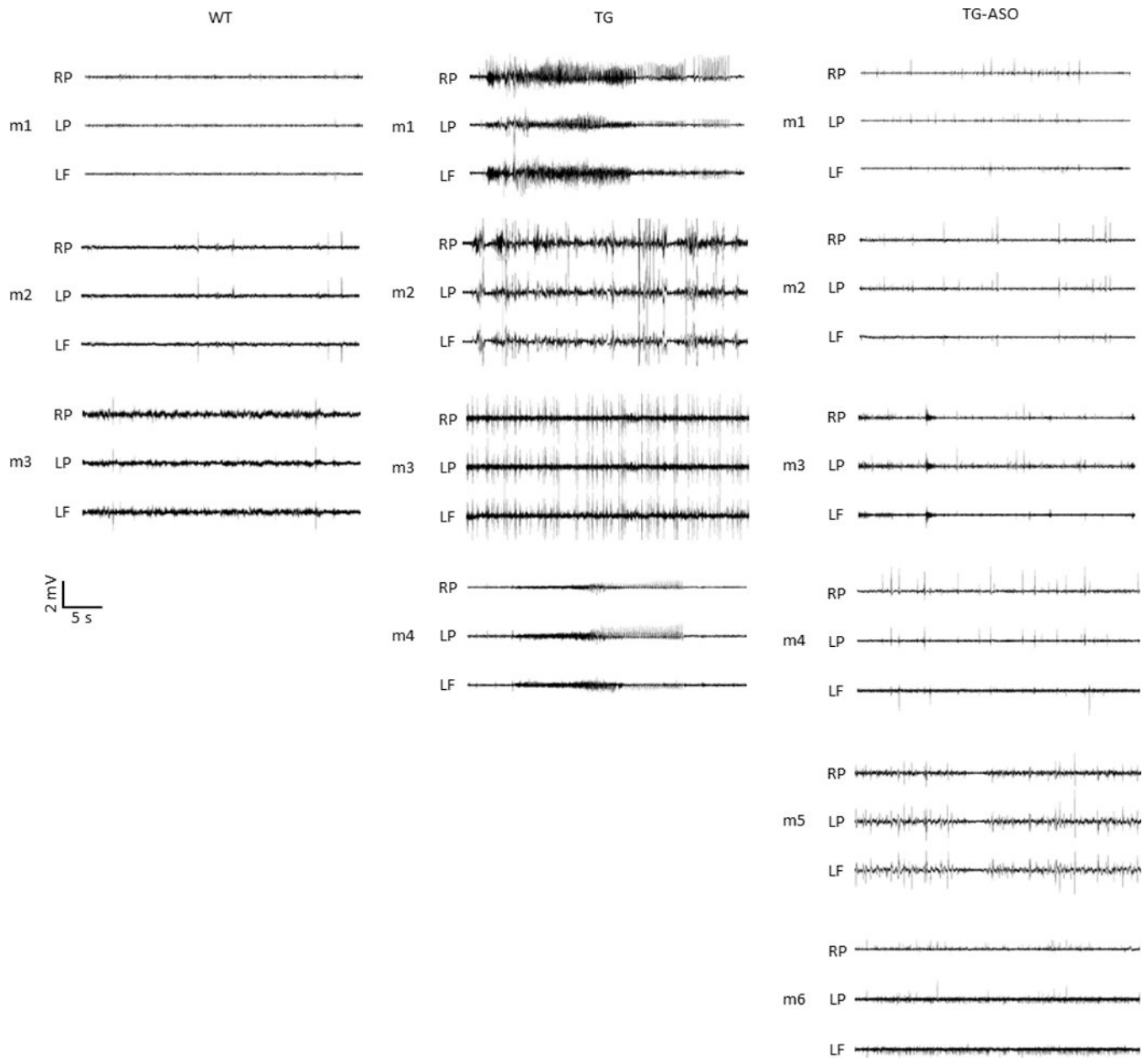
Extended Data figure 8. Cortical electroencephalogram (EEG) recording
Representative EEG traces of all mice recorded after gradual *MECP2*-ASO or control-ASO treatment. RP, right parietal cortex; LP, left parietal cortex; LF, left frontal cortex.

Extended Data Table 1
Antisense oligonucleotide sequences

This table describes the sequence, length, molecular weight, and type of chemical modification of the different *MECP2*-ASOs tested and the control-ASO.

ASO	Sequence	Length (bp)	Molecular weight (Da)	Chemistry
ASO-1	AACTCTCTCGGTCACGGGCG	20	7141.88	MOE gapmer
ASO-2	CACACTGACCTTTCAGGGCT	20	7100.87	MOE gapmer
ASO-3	GATCACTGGAACACAATGGT	20	7155.87	MOE gapmer
ASO-4	CGTGCCATGGAAGTCCTTCC	20	7116.87	MOE gapmer
ASO-5	GGTTTTTCTCCTTTATTATC	20	7035.77	MOE gapmer
Control-ASO	GTTTTCAAATACACCTTCAT	20	7045.82	MOE gapmer

Extended Data Table 2
Demographics of *MECP2* duplication syndrome patients

This table describes the demographics of the *MECP2* duplication patients and healthy donors that provided blood samples to establish immortalized B-lymphoblastoid cell lines. The last column on the right describes the individual *MECP2* mRNA expression levels in lymphoblasts, relative to the average of the healthy donors.

Subject ID	Date of birth	Date of collection	Age at collection (years)	Gender	*MECP2* expression fold change (relative to average control)
Control-1	07.10.1987	10.15.1992	5	Male	1.26
Control-2	08.22.1998	07.08.1999	1	Male	0.87
Control-3	07.13.2006	02.15.2013	6.7	Male	0.62
Control-4	11.17.2006	11.02.2012	6	Male	0.80
Control-5	06.23.2006	06.14.2013	7	Male	1.43
Duplication-1	04.11.2007	11.13.2008	1.5	Male	2.51
Duplication-2	11.07.2002	12.06.2007	5	Male	2.28
Duplication-3	10.25.2003	04.14.2008	4.5	Male	2.42
Duplication-4	02.02.1999	07.26.2006	7.5	Male	1.99
Duplication-5	11.01.2002	06.17.2008	5.5	Male	2.00

Supplementary Material

Refer to Web version on PubMed Central for supplementary material.

Acknowledgments

References

1. Malhotra D, Sebat J. CNVs: harbingers of a rare variant revolution in psychiatric genetics. Cell. 2012; 148:1223–1241. [PubMed: 22424231]

2. Lugtenberg D, et al. Structural variation in Xq28: MECP2 duplications in 1% of patients with unexplained XLMR and in 2% of male patients with severe encephalopathy. Eur J Hum Genet. 2009; 17:444–453. [PubMed: 18985075]

3. Van Esch H. MECP2 Duplication Syndrome. Molecular Syndromology. 2011

4. Ramocki MB, Tavyev YJ, Peters SU. The MECP2 duplication syndrome. Am J Med Genet A. 2010; 152A:1079–1088. [PubMed: 20425814]

5. Lubs H, et al. XLMR syndrome characterized by multiple respiratory infections, hypertelorism, severe CNS deterioration and early death localizes to distal Xq28. Am J Med Genet. 1999; 85:243–248. [PubMed: 10398236]

6. Costa RM, et al. Mechanism for the learning deficits in a mouse model of neurofibromatosis type 1. Nature. 2002; 415:526–530. [PubMed: 11793011]

7. Ehninger D, et al. Reversal of learning deficits in a Tsc2+/− mouse model of tuberous sclerosis. Nat Med. 2008; 14:843–848. [PubMed: 18568033]

8. Dolen G, et al. Correction of fragile X syndrome in mice. Neuron. 2007; 56:955–962. [PubMed: 18093519]

9. Guy J, Gan J, Selfridge J, Cobb S, Bird A. Reversal of neurological defects in a mouse model of Rett syndrome. Science. 2007; 315:1143–1147. [PubMed: 17289941]

10. Southwell AL, Skotte NH, Bennett CF, Hayden MR. Antisense oligonucleotide therapeutics for inherited neurodegenerative diseases. Trends Mol Med. 2012; 18:634–643. [PubMed: 23026741]

11. Bennett CF, Swayze EE. RNA targeting therapeutics: molecular mechanisms of antisense oligonucleotides as a therapeutic platform. Annu Rev Pharmacol Toxicol. 2010; 50:259–293. [PubMed: 20055705]

12. Lentz JJ, et al. Rescue of hearing and vestibular function by antisense oligonucleotides in a mouse model of human deafness. Nat Med. 2013; 19:345–350. [PubMed: 23380860]

13. Wheeler TM, et al. Targeting nuclear RNA for in vivo correction of myotonic dystrophy. Nature. 2012; 488:111–115. [PubMed: 22859208]

14. Hua Y, et al. Peripheral SMN restoration is essential for long-term rescue of a severe spinal muscular atrophy mouse model. Nature. 2011; 478:123–126. [PubMed: 21979052]

15. Meng L, et al. Towards a therapy for Angelman syndrome by targeting a long non-coding RNA. Nature. 2014

16. Kordasiewicz HB, et al. Sustained therapeutic reversal of Huntington's disease by transient repression of huntingtin synthesis. Neuron. 2012; 74:1031–1044. [PubMed: 22726834]

17. Passini MA, et al. Antisense oligonucleotides delivered to the mouse CNS ameliorate symptoms of severe spinal muscular atrophy. Sci Transl Med. 2011; 3:72ra18.

18. Smith RA, et al. Antisense oligonucleotide therapy for neurodegenerative disease. J Clin Invest. 2006; 116:2290–2296. [PubMed: 16878173]

19. Collins AL, et al. Mild overexpression of MeCP2 causes a progressive neurological disorder in mice. Hum Mol Genet. 2004; 13:2679–2689. [PubMed: 15351775]

20. Samaco RC, et al. Crh and Oprm1 mediate anxiety-related behavior and social approach in a mouse model of MECP2 duplication syndrome. Nat Genet. 2012; 44:206–211. [PubMed: 22231481]

21. Chahrour M, et al. MeCP2, a key contributor to neurological disease, activates and represses transcription. Science. 2008; 320:1224–1229. [PubMed: 18511691]

22. Ben-Shachar S, Chahrour M, Thaller C, Shaw CA, Zoghbi HY. Mouse models of MeCP2 disorders share gene expression changes in the cerebellum and hypothalamus. Hum Mol Genet. 2009; 18:2431–2442. [PubMed: 19369296]

23. Chao HT, et al. Dysfunction in GABA signalling mediates autism-like stereotypies and Rett syndrome phenotypes. Nature. 2010; 468:263–269. [PubMed: 21068835]

24. Lewis JD, et al. Purification, sequence, and cellular localization of a novel chromosomal protein that binds to methylated DNA. Cell. 1992; 69:905–914. [PubMed: 1606614]

25. Nan X, et al. Transcriptional repression by the methyl-CpG-binding protein MeCP2 involves a histone deacetylase complex. Nature. 1998; 393:386–389. [PubMed: 9620804]

26. Jones PL, et al. Methylated DNA and MeCP2 recruit histone deacetylase to repress transcription. Nat Genet. 1998; 19:187–191. [PubMed: 9620779]

27. Chao HT, Zoghbi HY. MeCP2: only 100% will do. Nat Neurosci. 2012; 15:176–177. [PubMed: 22281712]

28. Patel PI, et al. The gene for the peripheral myelin protein PMP-22 is a candidate for Charcot-Marie-Tooth disease type 1A. Nat Genet. 1992; 1:159–165. [PubMed: 1303228]

29. Potocki L, et al. Characterization of Potocki-Lupski syndrome (dup(17)(p11.2p11.2)) and delineation of a dosage-sensitive critical interval that can convey an autism phenotype. Am J Hum Genet. 2007; 80:633–649. [PubMed: 17357070]

30. Arron JR, et al. NFAT dysregulation by increased dosage of DSCR1 and DYRK1A on chromosome 21. Nature. 2006; 441:595–600. [PubMed: 16554754]

References

31. Cook MN, Williams RW, Flaherty L. Anxiety-related behaviors in the elevated zero-maze are affected by genetic factors and retinal degeneration. Behav Neurosci. 2001; 115:468–476. [PubMed: 11345971]

32. Kim D, et al. TopHat2: accurate alignment of transcriptomes in the presence of insertions, deletions and gene fusions. Genome Biol. 2013; 14:R36. [PubMed: 23618408]

33. Anders S, Pyl PT, Huber W. HTSeq--a Python framework to work with high-throughput sequencing data. Bioinformatics. 2015; 31:166–169. [PubMed: 25260700]

34. Anders S, Huber W. Differential expression analysis for sequence count data. Genome Biol. 2010; 11:R106. [PubMed: 20979621]

35. Paxinos, G.; Franklin, KB. The mouse brain in stereotaxic coordinates. San Diego: Academic; 2001.

36. Han K, et al. SHANK3 overexpression causes manic-like behaviour with unique pharmacogenetic properties. Nature. 2013; 503:72–77. [PubMed: 24153177]

37. Roberson ED, et al. Amyloid-beta/Fyn-induced synaptic, network, and cognitive impairments depend on tau levels in multiple mouse models of Alzheimer's disease. J Neurosci. 2011; 31:700–711. [PubMed: 21228179]
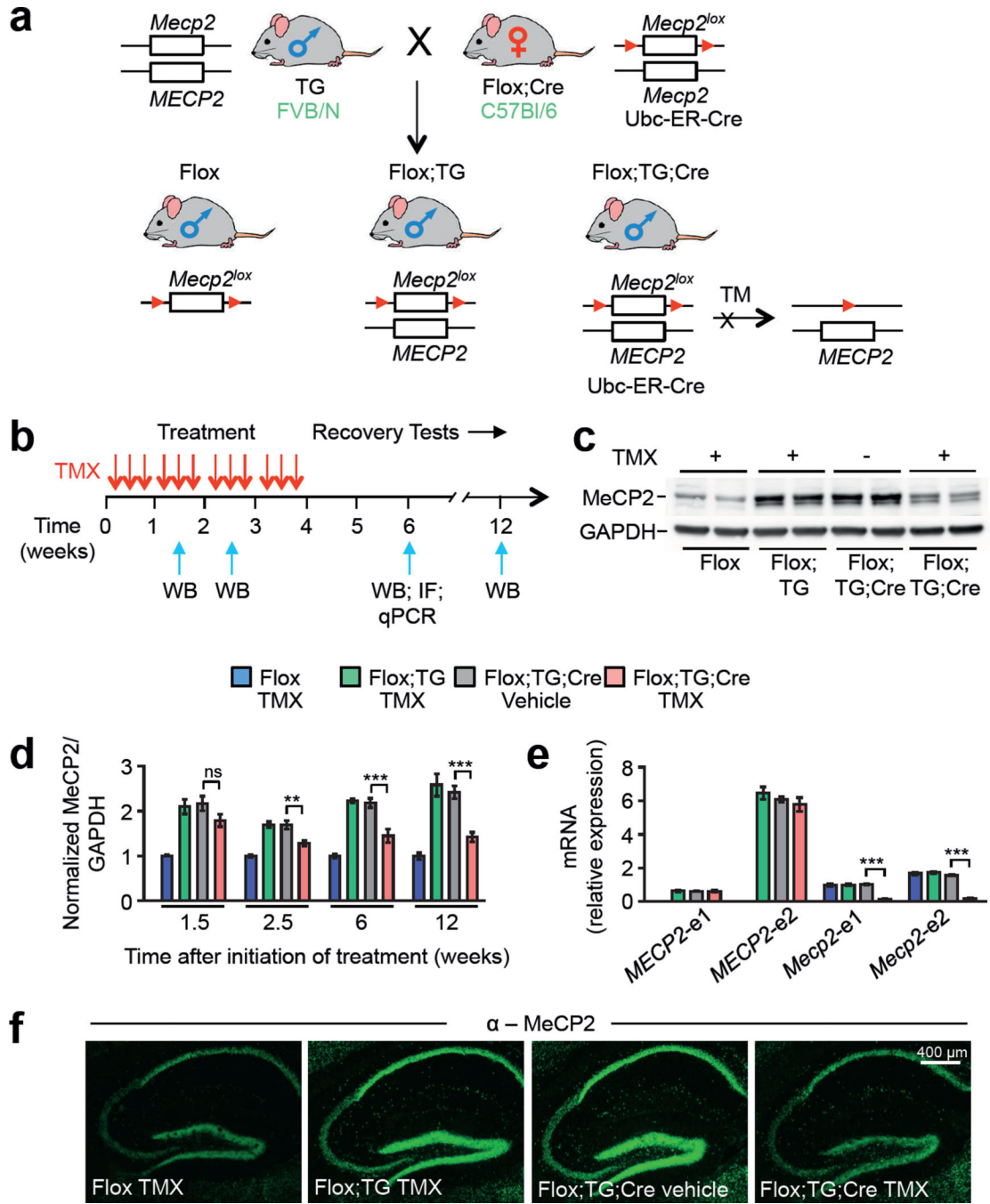
Figure 1. Inducible Cre-lox recombination normalizes MeCP2 levels in adult *MECP2* duplication mice

a, Breeding strategy to generate conditional *MECP2* overexpression mice. **b**, Tamoxifen (TMX) treatment protocol and the time points for western blot (WB), immunofluorescence (IF) and RT-qPCR. **c**, WB from cortical samples at 6 weeks (for gel source data, see Supplementary Figure 1). **d**, Kinetics of MeCP2 levels (n = 6, two-tailed *t*-test; for gel source data, see Supplementary Figure 1). **e**, RT-qPCR from cortical samples with specific primers for human or mouse *Mecp2*, and for each of the two alternatively spliced isoforms

(n = 6, two-tailed *t*-test). **f**, Immunostaining for MeCP2 in hippocampal slices. ns, not significant. Data are presented as mean ± s.e.m. ** $P < 0.01$; ***$P < 0.001$.
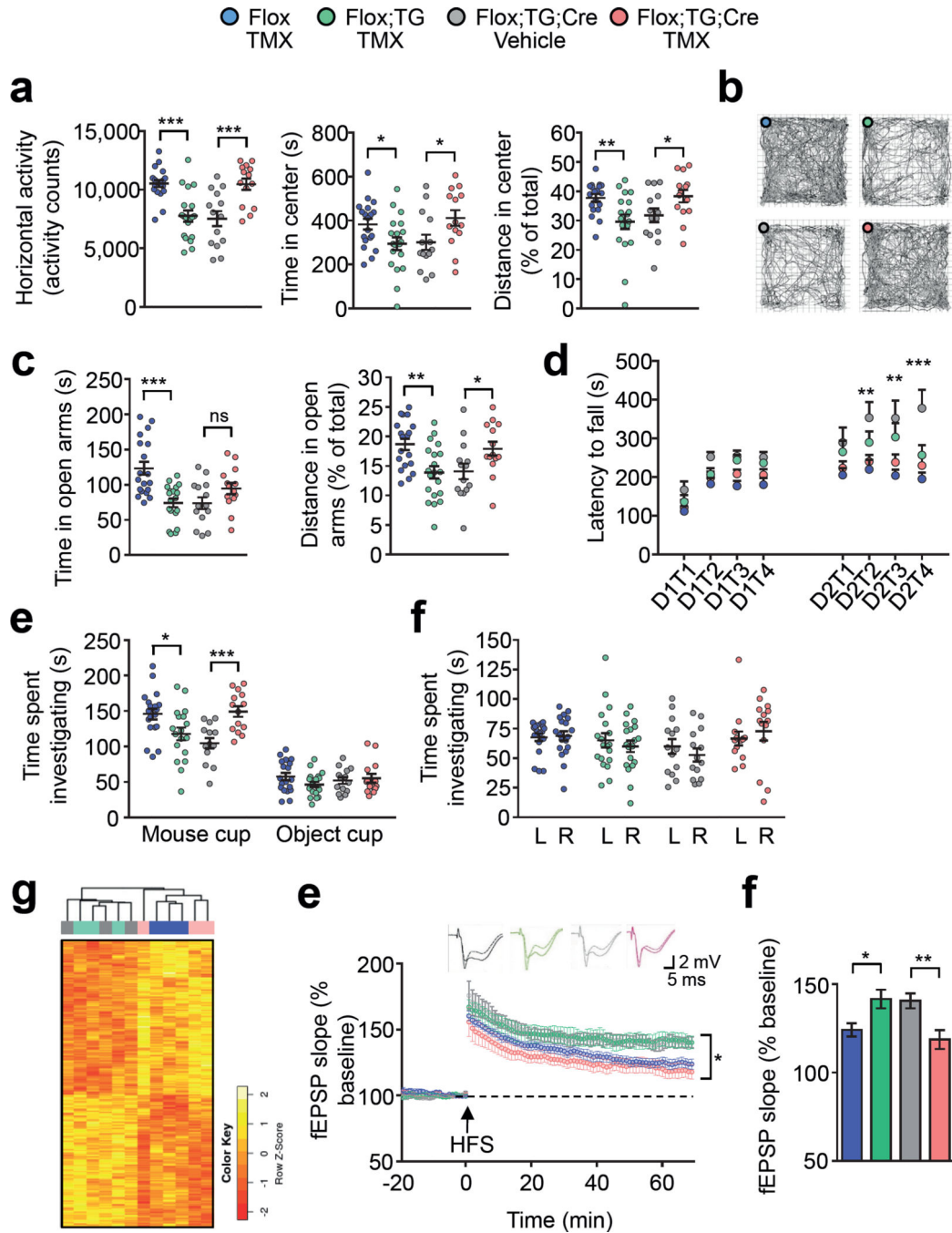
Figure 2. Genetic normalization of MeCP2 levels reverses deficits in adult *MECP2* duplication mice

a, Reversal of hypoactivity and anxiety-like behaviors in the open field. **b**, Representative tracking plots of the open field. **c**, Reversal of anxiety-like behavior in the elevated plus maze. **d**, Reversal of abnormal motor behavior on the rotarod (asterisks indicate significance between Flox;TG;Cre-TMX and Flox;TG;Cre-vehicle groups). D1T1, day 1/trial 1. **e**, Reversal of social behavior in the 3-chamber test. **f**, No preference for the left (L) or right (R) chambers in the habituation phase of the test. n = 19 for Flox-TMX and Flox;TG-TMX

groups. n = 14 for Flox;TG;Cre-vehicle and Flox;TG;Cre-TMX groups. **g**, Transcriptional heat map for the hippocampus (n = 3). **e**, TMX treatment normalized LTP in Flox;TG;Cre mice (n = 6–7 mice/15–20 slices, two-way ANOVA repeated measures followed by Tukey HSD *post hoc* correction for multiple comparisons). Top: representative electrophysiological traces at baseline and after stimulation. **f**, Quantification of the last 10 minutes of the LTP recording (n = 6–7 mice/15–20 slices, two-tailed *t*-test). Behavioral data were analyzed by two-tailed *t*-test except for the rotarod, which was analyzed by two-way ANOVA repeated measures followed by Tukey HSD *post hoc* correction for multiple comparisons. Data are presented as mean ± s.e.m. *$P < 0.05$; ** $P < 0.01$; ***$P < 0.001$.

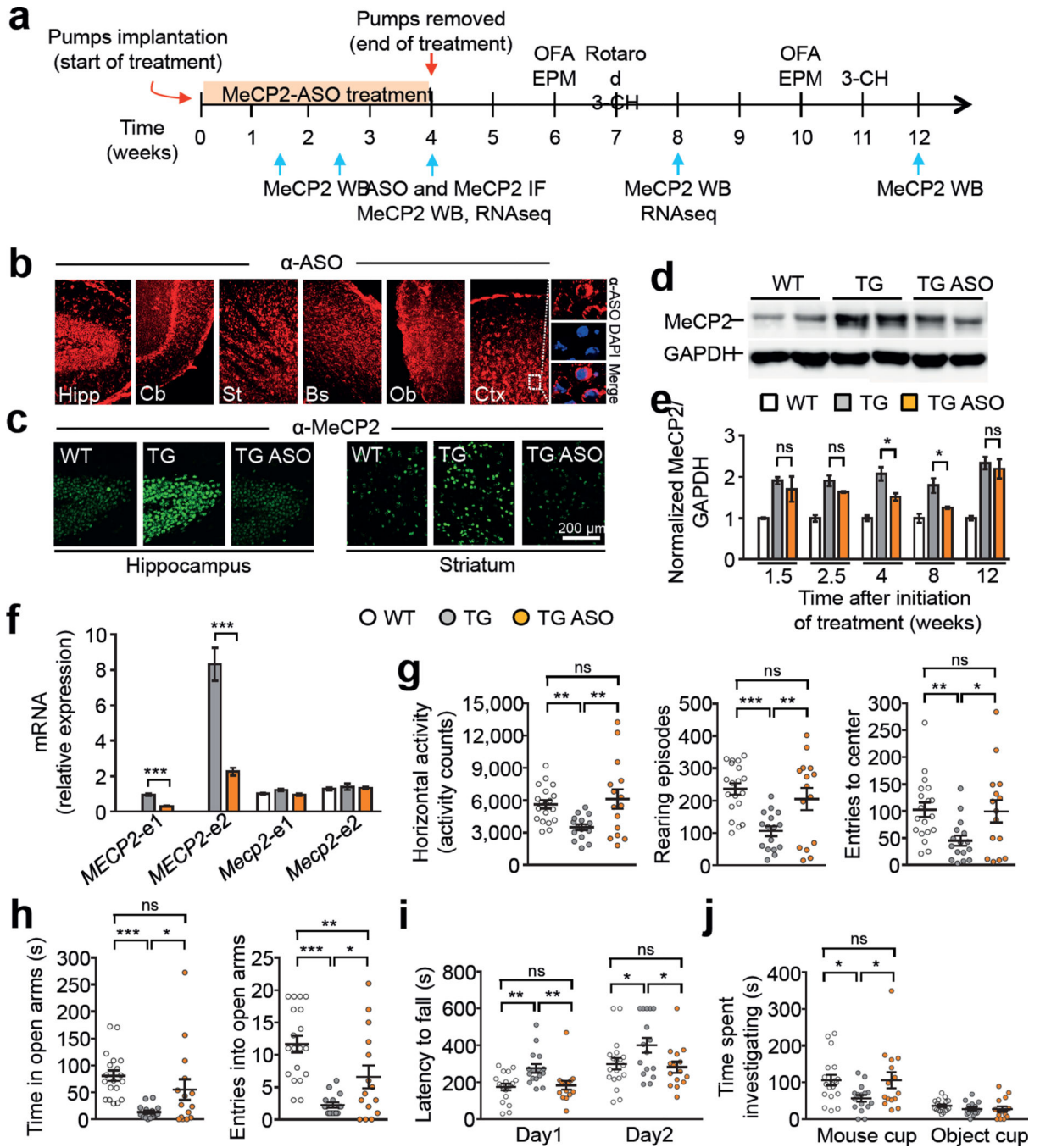**Figure 3. Gradual infusion of ASO normalizes MeCP2 levels and reverses abnormal behavior**
a, Timeline of gradual ASO treatment and western blot (WB), immunofluorescence (IF), RNA-seq and behavioral tests. OFA, open field activity; EPM, elevated plus maze; 3-CH, 3 chamber. **b**, Immunofluorescence staining against ASOs. Hipp, hippocampus; Cb, cerebellum; St, striatum; Bs, brainstem; Ob, olfactory bulb; Ctx, cortex. **c**, Immunofluorescence staining for MeCP2. **d**, Representative WB of MeCP2 in the cortex 4 weeks after initiation of treatment (for gel source data, see Supplementary Figure 2). **e**, Kinetics of MeCP2 levels (n = 4–5, two-tailed t-test; for gel source data, see Supplementary

Figure 2). **f**, RT-qPCR from cortical samples with specific primers for mouse or human *MECP2* and for each of the two alternatively spliced *MECP2* isoforms (n = 3, two-tailed *t*-test). **g**, Reversal of hypoactivity and anxiety-like behavior in the open field at week 10. **h**, Reversal of anxiety-like behavior in the elevated plus maze at week 10. **i**, Reversal of abnormal motor behavior on the rotarod at week 7. Data were averaged per day over 4 trials. **j**, Reversal of abnormal social behavior in the 3-chamber test at week 11. All behavioral data were analyzed by one-way ANOVA followed by Fisher's LSD *post hoc* test. n = 19 for WT group; n = 16 for TG group; n = 15 for TG-ASO group. ns, not significant. Data are presented as mean ± s.e.m. $*P < 0.05$; $** P < 0.01$; $***P < 0.001$.
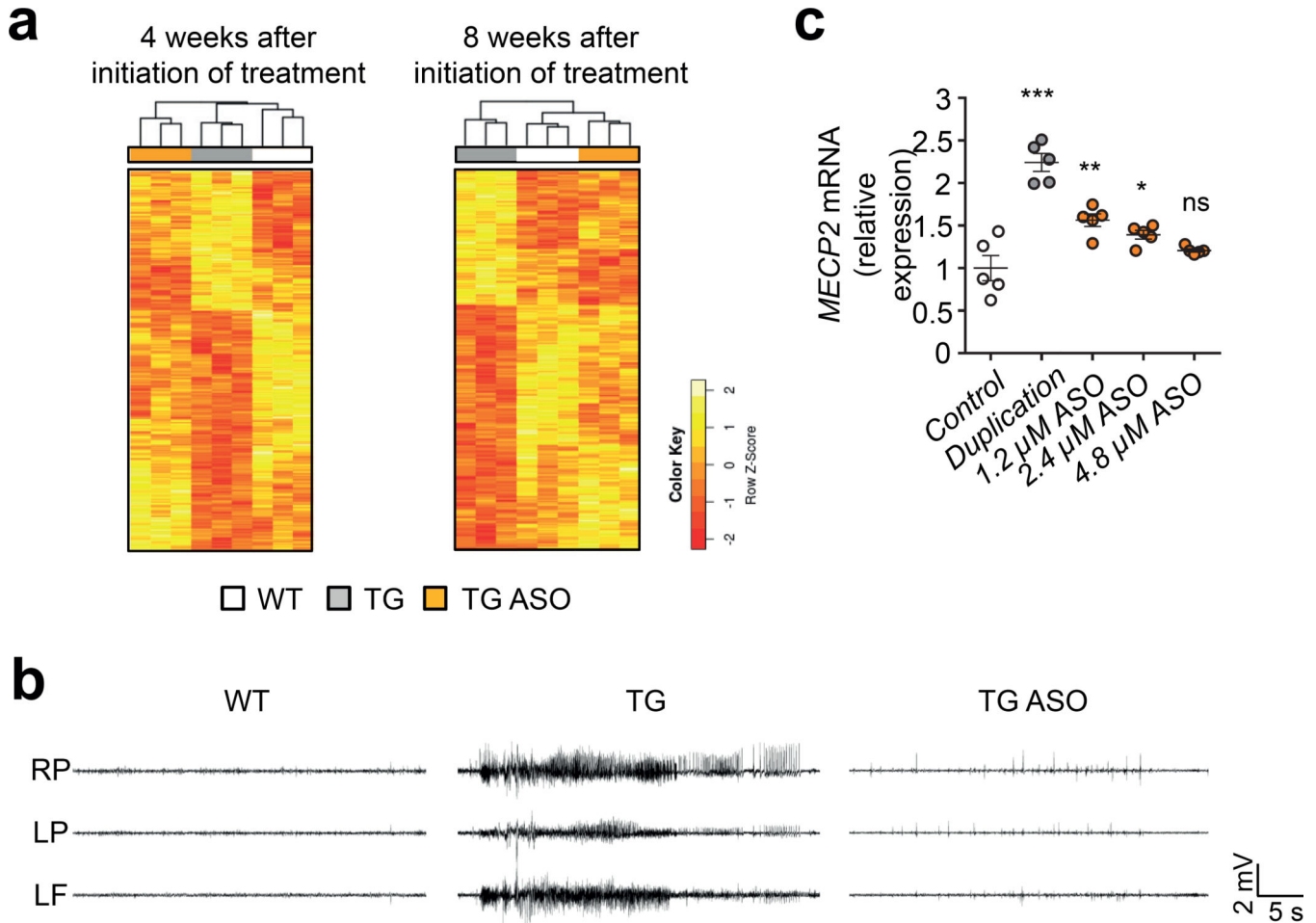
Figure 4. ASO treatment corrects abnormal gene expression and EEG

a, Transcriptional heat maps of the hippocampus (n = 3 mice per group). **b**, Representative EEG traces (n = 3 for WT, n = 4 for TG, n = 6 for TG-ASO). RP, right parietal cortex; LP, left parietal cortex; LF, left frontal cortex. **c**, ASO corrected *MECP2* mRNA levels in lymphoblastoid cells from *MECP2* duplication patients (n = 5, one-way ANOVA followed by Tukey HSD *post hoc* correction for multiple comparisons. Asterisks denote statistical difference to the control group). ns, not significant. Data are presented as mean ± s.e.m. *$P < 0.05$; ** $P < 0.01$; ***$P < 0.001$.